On-chip optical pulse shaper for arbitrary waveform generation*

Liao Sha-Sha(廖莎莎), Yang Ting(杨 婷), and Dong Jian-Ji(董建绩)†

Wuhan National Laboratory for Optoelectronics,School of Optoelectronic Science and Engineering, Huazhong University of Science and Technology, Wuhan 430074, *China*

(Received 15 November 2013; revised manuscript received 6 January 2014; published online 28 May 2014)

We propose and demonstrate a silicon-on-insulator (SOI) on-chip optical pulse shaper based on four-tap finite impulse response. Due to different width designs in phase region of each tap, the phase differences for all taps are controlled by an external thermal source, resulting in an optical pulse shaper. We further demonstrate optical arbitrary waveform generation based on the optical pulse shaper assisted by an optical frequency comb injection. Four different optical waveforms are generated when setting the central wavelengths at 1533.78 nm and 1547.1 nm and setting the thermal source temperatures at 23 °C and 33 °C, respectively. Our scheme has distinct advantages of compactness, capability for integrating with electronics since the integrated silicon waveguide is employed.

Keywords: pulse shaping, optical arbitrary waveform generation, silicon photonics, microwave photonics

PACS: 32.30.Bv, 42.79.Gn, 42.79.Sz **DOI:** 10.1088/1674-1056/23/7/073201

1. Introduction

Arbitrary waveform generation is very useful in testing and optimizing communication system, radar and signal processing,[1] such as generating ultra-wide band (UWB) signal[2,3] and all-optical temporal differentiator.[4,5] The methods of generating arbitrary waveforms can be divided into two categories, one is direct temporal shaping, which is based on the finite impulse response (FIR) model in the discrete time signal processing theory and the other is frequency shaping.The schemes of the two methods have been reported in recent years. A widely adopted approach based on frequency shaping is first to use a spectral disperser to separate the input optical frequency comb, and then use a modulator array to modulate the phase and amplitude of each line.[6,7] The spectral disperser can be a grating[8] or a microring.[9] The modulator array can be acousto-optic modulators,[10] microring array,[9] or liquid crystal modulator array.[11–14] Although these schemes have shown flexibility in reconfiguration,[15] and they can realize line-by-line shaping with high resolution and wide bandwidth,[16,17] the complexity of the configuration and the high loss of the coupling restrict their extensive applications.[18] Although some schemes using integrated devices (usually microrings[19,20]) can overcome the above drawbacks. The systems still become very complex when the ideal waveform is intricate. On the other hand, the direct temporal shaping is used to control the time delays and the amplitudes of the multipath pulses to directly generate arbitrary waveform in time domain.[1,21,22] It is convenient to generate a complex waveform by this method. However, the generated waveforms are synthetized with the amplitude of each tap, regardless of phase.

In this paper, we propose and demonstrate a silicon monolithic integrated optical pulse shaper based on four-tap finite impulse response. By thermally controlling the phase region of each tap, an optical pulse shaper is obtained. With the assistance of an optical frequency comb injection, four different optical waveforms are generated when setting the central wavelength at 1533.78 nm and 1547.1 nm and setting the thermal source at 23 °C and 33 °C, respectively. Our scheme has distinct advantages of compactness, capability for integrating with electronics since the integrated silicon waveguide is employed.

2. Operation principle

The principle of the integrated optical pulse shaper is based on FIR of four taps. The pattern structure is monolithic integrated on a silicon-on-insulator wafer, and has the advantages of easy fabrication and compact footprint. For an ideal pulse shaper fabricated with temporal synthesis method, both the phase and amplitude of all taps should be adjusted independently. For simplicity here, we only design the phase modulation region with variable waveguide widths for each tap. The schematic of the integrated optical pulse shaper is shown in Fig. 1. The input signal is divided into four paths by the cascaded Y-branches. There is a phase modulation region on each path. It is known that the silicon reflective index varies with temperature, leading to the change of phase. The phase variations of four taps are totally different at the same temperature if the waveguide widths are different. Thus, heating a series

*Project supported by the National Basic Research Program of China (Grant No. 2011CB301704), the Program for New Century Excellent Talents in Ministry of Education of China (Grant No. NCET-11-0168), the Foundation for the Author of National Excellent Doctoral Dissertation of China (Grant No. 201139), and the National Natural Science Foundation of China (Grant Nos. 60901006 and 11174096).

†Corresponding author. E-mail: jjdong@mail.hust.edu.cn

© 2014 Chinese Physical Society and IOP Publishing Ltd

of waveguides with distinct widths can implement an optical pulse shaper.

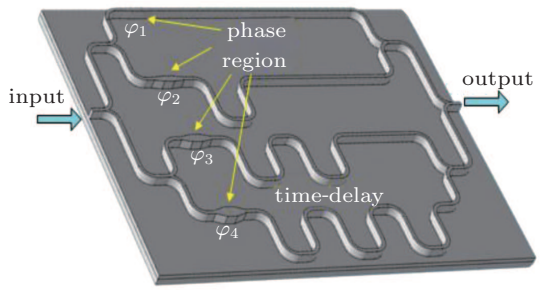


Fig. 1. (color online) Schematic diagram of integrated optical pulse shaper.

Assuming that the phases of the four paths are φ_1, φ_2, φ_3 and φ_4, respectively, and the time delay between two adjacent taps is τ, the transfer function of the optical pulse shaper can be expressed as

$$H(f) = \sum_{n=1}^{4} \mathrm{e}^{\mathrm{j}(2\pi f n\tau + \phi_n)}. \tag{1}$$

Equation (1) indicates that the output spectrum can be reshaped by modifying the phase array of the four taps. Assume that the time delay between these four taps is increased by 30 ps in sequence. The simulated spectra of the optical pulse shaper with different phase arrays (φ_1, φ_2, φ_3, φ_4) are shown in Fig. 2, where Figs. 2(a)–2(d) are the simulated spectra when the phase arrays are set with (0, 0, 0, 0), (0, π/2, π, 3π/2), (0, 0, π, π), and (0, π, 0, π), respectively. We can see that the output spectrum changes with phase setting for each of the four taps, revealing a pulse shaper. We can then use this optical pulse shaper to implement arbitrary waveform generation.

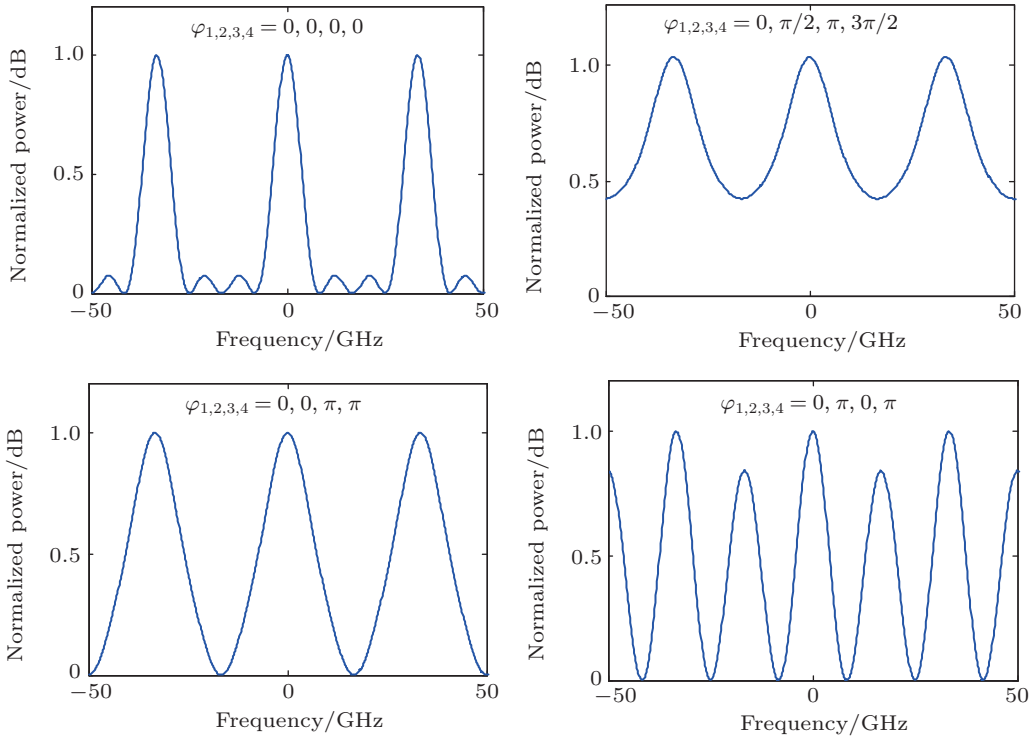


Fig. 2. (color online) Simulated spectra of the pulse shaper with phase arrays being (a) (0, 0, 0, 0), (b) (0, π/2, π, 3π/2), (c) (0, 0, π, π), and (d) (0, π, 0, π).

3. Experimental demonstration and discussion

First, we make a layout design for the silicon integrated pulse shaper, as shown in Fig. 1. In the process of device fabrication, the pulse shaper is fabricated on an SOI wafer (340 nm thick silicon on 2-μm-thick silica). The height of the waveguide is 240 nm and the width of the waveguide is 617 nm. The radius of each Y branch is 20 μm. The widths of the four phase modulation regions are 0.617 μm, 0.669 μm, 0.748 μm and 0.845 μm, respectively. The time delay of the four taps is increased by 12.5 ps successively. E-beam lithography (Vistec EBPG 5000 Plus) is used to determine the pattern of pulse shaper on the ZEP520A resist. The pattern is then transferred to the top silicon layer by inductively coupled plasma (ICP) etching using SF_6 and C_4F_8 gases. Figure 3(a) shows the metallurgical microscopy image of the pulse shaper, Figures 3(b)–3(d) show scanning electron microscope (SEM) images of the phase region, grating coupler and Y branch, respectively. A clear pattern can be observed in our device fabrication.

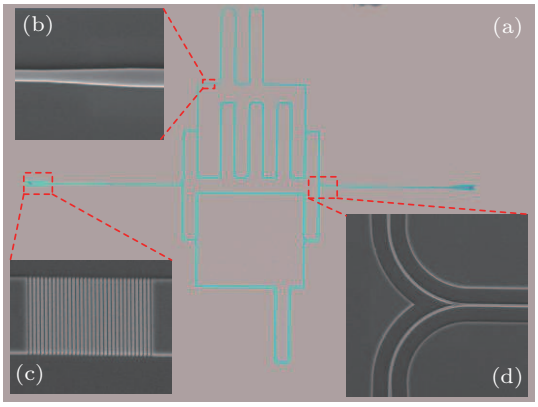


Fig. 3. (color online) Metallurgical microscopy image of (a) pulse shaper, and SEM images of (b) phase region, (c) grating coupler, and (d) Y branch.

The measured transmission of the integrated optical pulse shaper is shown in Fig. 4. The loss of the shaper is about 20 dB and the loss of the coupling from the grating to fiber is about 18.5 dB. In order to monitor different spectral transmissions, we may change the chip temperature or observe the transmissions in different spectral ranges. The transmission of pulse shaper varies with temperature because of different widths for the four taps. On the other hand, the silicon refractive index is also related to the incident wavelength. Therefore, the transmissions in different spectral ranges may be different even at the same temperature operation. Figures 4(a) and 4(b) show the transmissions (solid line) of the integrated chip operating at 23 °C when the central wavelengths are 1533.78 nm and 1547.1 nm, respectively (the origin point of the horizontal axis presents 1533.78 nm and 1547.1 nm, unless otherwise stated). We employ Fourier transformation theory to retrieve the phases and amplitudes of four taps on the chip, and then simulate the spectral transmission (dashed line) for comparison. In Fig. 4(a), the calculated phase array for the four taps is (0, π, 0, π), and the calculated amplitude array is (1, 0.13, 0.13, 0.6). We notice that the amplitude distributions for the four taps are not the same as we expect. The power unbalance results from the non-uniform thermal conductivity and the device fabrication deviations. In Fig. 4(b), the calculated phase array for the four taps is (0, π, -0.1π, π), and the calculated amplitude array is (1, 0.47, 0.1, 0.12). Similarly, the chip temperature is increased to 33 °C, and the transmission spectra are shown in Figs. 4(c) and 4(d) when the central wavelengths are 1533.78 nm and 1547.1 nm, respectively. Here, we observe a totally different transmission. Then, the calculated phase array and amplitude array for Fig. 4(c) are (0, 0.8π, 0.24π, π) and (1, 0.4, 0.28, 0.51), respectively. For Fig. 4(d), the phase array and the amplitude array are (0, π, 0.04π, π) and (1, 0.4, 0.1, 0.3), respectively. To implement optical arbitrary waveform generation, we may change the spectral range or the temperature of chips.

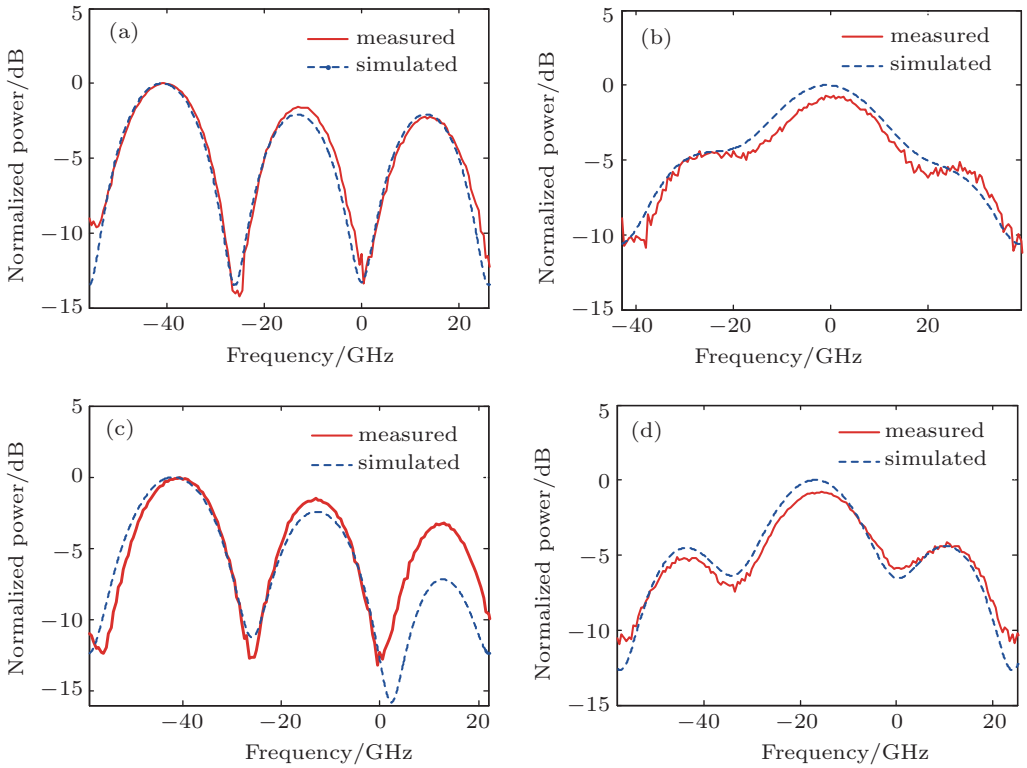


Fig. 4. (color online) Measured and simulated transfer function of the optical pulse shaper in the four different cases: (a) the temperature of the chip is 23 °C and the central wavelength is 1533.78 nm, (b) the temperature of the chip is 23 °C and the central wavelength is 1547.1 nm, (c) the temperature of the chip is 33 °C and the central wavelength is 1533.78 nm, (d) the temperature of the chip is 33 °C and the central wavelength is 1547.1 nm.

The experimental setup for optical arbitrary waveform generation is shown in Fig. 5. In order to create an optical frequency comb, a continuous wave (CW) light is emitted from the tunable laser diode (TLD) with a precisely tuning resolution of 100 MHz. The light is modulated by the Mach–Zehnder modulator (MZM) and phase modulator (PM), which are driven by a tunable radio frequency (RF) signal (20 GHz initially). Because of the polarization sensitivity, there are two polarization controllers (PCs) placed before the MZM and PM. A 9-km single mode fiber (SMF) is used to compensate the incident chirps to generate more and flatter optical frequency comb lines. By using this optical frequency comb generator, we can achieve almost 50 spectral lines (the 3 dB bandwidth of the pulse is 20.7 ps). As shown in Fig. 2, the transmission spectrum of the integrated chip is periodical due to the FIR filter. Hence, a tunable optical band-pass filter (OBF) is used to pick out one period of the spectrum of the silicon chip. In this experiment we use two vertical grating couplers to couple the light from fiber to silicon waveguide and the output signal from waveguide to fiber. A PC is placed before the first grating coupler because the coupler is polarization dependent. A ceramic heater is placed under the chip to heat the entire chip, thus the chip temperature is adjustable. Then, the phase of each tap can be varied. Finally the output temporal waveform is measured by a high speed oscilloscope (OSC) with a bandwidth of 500 GHz (Eye-Checker 1000C).

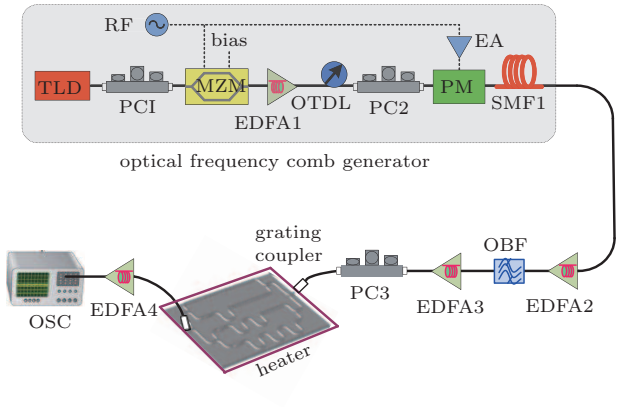


Fig. 5. (color online) Experimental setup of the arbitrary waveform generation with employing the integrated chip.

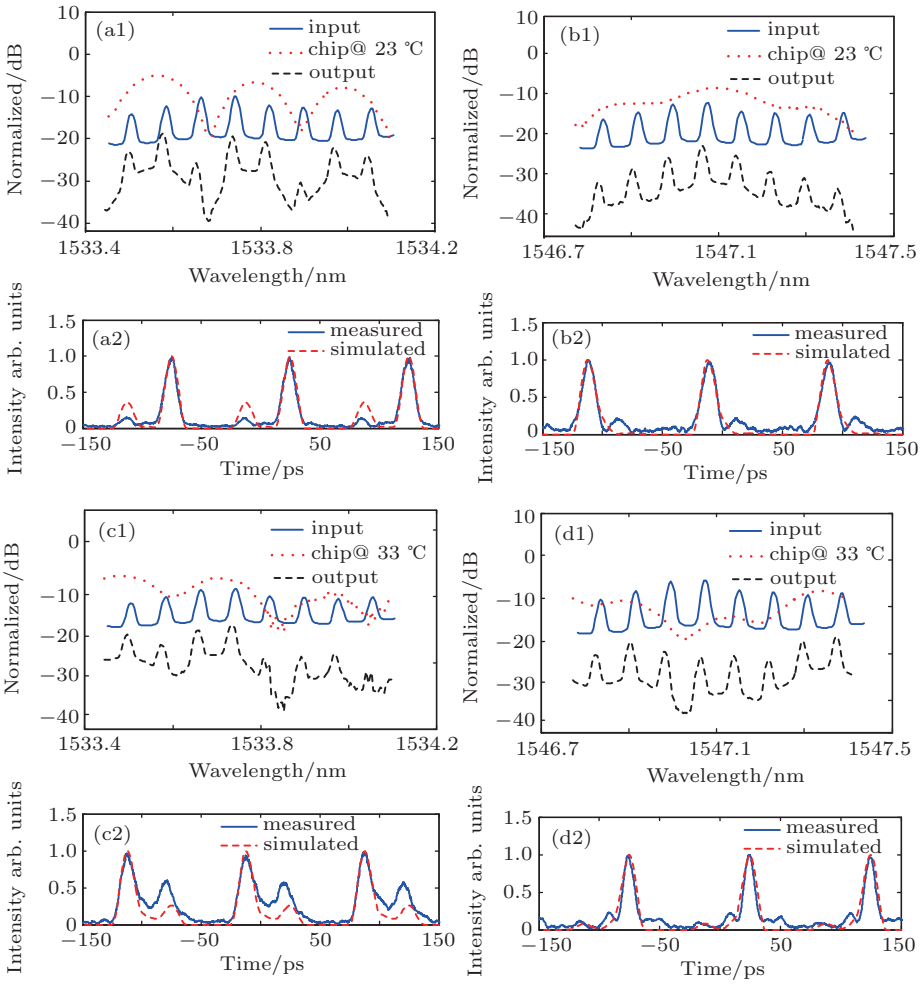


Fig. 6. (color online) Measured spectra, measured and simulated waveforms of the optical pulse shaper, (a1), (b1), (c1), (d1) show the spectra of the optical frequency comb, transfer function of the optical pulse shaper and the spectrum of the output signal at different temperatures and center wavelengths, (a2), (b2), (c2), (d2) show the measured (solid line) and simulated (dashed line) output waveforms at different temperatures and central wavelengths, respectively.

At first, the chip temperature is kept at 23 °C. The wavelength of the CW light is 1533.78 nm. The OBF is used to filter out one period of the transmission spectrum of the chip, and the central wavelength is 1533.78 nm. Figure 6(a1) shows the spectral evolution, where the solid line represents the input optical frequency comb, and dotted line represents the chip transmission, and dashed line represents the output spectrum. The measured (solid line) and simulated (dashed line) output temporal waveforms are shown in Fig. 6(a2). Similarly, figures 6(b1) and 6(b2) show another spectral evolution and output waveform when the central wavelength is changed into 1547.10 nm. Then the chip temperature is increased to 33 °C, and we repeat the spectrum and waveform measurements. Figures 6(c1) and 6(c2) show spectral evolutions and output waveforms when the central wavelength is changed into 1533.78 nm. Figures 6(d1) and 6(d2) show another spectrum and waveform with central wavelength aligned to 1547.10 nm. Comparing these four different waveforms, we can see that the output waveform can be changed by heating/cooling the chip or taking different spectral ranges of the transmission. Therefore, we can implement optical arbitrary waveform generation using this integrated pulse shaper.

It should be noted that we have demonstrated only a simplified optical pulse shaper. For a complete optical pulse shaper with FIR, both phase and amplitude of each of all taps should be adjusted independently. We can use an independent thermal heater in each phase region to control the phase precisely and add a Mach–Zehnder interferometer (MZI) structure with independent thermal modulation on each tap to control the amplitude of the signal. Then, we can obtain more precise arbitrary waveform. In order to reduce the loss of the shaper, we can optimize the coupling grating and use thermal oxidation to reduce the surface roughness.

4. Conclusion

We propose and demonstrate an on-chip optical pulse shaper based on four-tap FIR. We further demonstrate optical arbitrary waveform generation based on the optical pulse shaper with the assistance of an optical frequency comb injection. Four different optical waveforms are generated when setting the central wavelengths at 1533.78 nm and 1547.1 nm and setting the thermal source temperatures at 23 °C and 33 °C, respectively. We demonstrate that this scheme can realize arbitrary waveform generation.

References

[1] Shen M and Minasian R A 2004 *IEEE Photonic Tech. L* **16** 1155
[2] Luo B W, Dong J J, Yu Y, Yang T and Zhang X L 2013 *Chin. Phys. B* **22** 023201
[3] Dong J J, Luo B W, Huang D X and Zhang X L 2012 *Chin. Phys. B* **21** 043201
[4] Dong J J, Luo B W, Zhang Y, Lei L, Huang D X and Zhang X L 2012 *Chin. Phys. Lett.* **29** 014203
[5] Zheng A L, Dong J J, Lei L, Yang T and Zhang X L 2013 *Chin. Phys. B* **23** 033201
[6] Weiner A M 2011 *Opt. Commun.* **284** 3669
[7] Wang N, Han H N, Li D H and Wei Z Y 2012 *Acta Phys. Sin.* **61** 184201 (in Chinese)
[8] Fang X, Wang D N and Li S 2003 *JOSA B* **20** 1603
[9] Khan M H, Shen H, Xuan Y, Zhao L, Xiao S, Leaird D E, Weiner A M and Qi M 2010 *Nat. Photon.* **4** 117
[10] Dugan M, Tull J and Warren W 1997 *JOSA B* **14** 2348
[11] McKinney J, Leaird D and Weiner A 2002 *Opt. Lett.* **27** 1345
[12] Weiner A M, Leaird D E, Patel J S and Wullert J R 1990 *Opt. Lett.* **15** 326
[13] Weiner A M, Leaird D E, Patel J S and Wullert J R 1992 *IEEE J. Sel. Top. Quant.* **28** 908
[14] Wefers M M and Nelson K A 1995 *Opt. Lett.* **20** 1047
[15] Jiang Z, Huang C B, Leaird D E and Weiner A M 2007 *Nat. Photon.* **1** 463
[16] Supradeepa V, Huang C B, Leaird D E and Weiner A M 2008 *Opt. Express* **16** 11878
[17] Torres-Company V, Metcalf A J, Leaird D E and Weiner A M 2012 *IEEE Photonic Tech. L* **24** 891
[18] Zhang A and Li C 2013 *Opt. Laser Technol.* **52** 81
[19] Vantrease D, Schreiber R, Monchiero M, McLaren M, Jouppi N P, Fiorentino M, Davis A, Binkert N, Beausoleil R G and Ahn J H 2008 *ACM Comp. Ar.* **36** 153
[20] Batten C, Joshi A, Orcutt J, Khilo A, Moss B, Holzwarth C W, Popovic M A, Li H, Smith H I and Hoyt J L 2009 *IEEE Micro* **29** 8
[21] Wang S, Ciftcioglu B and Wu H 2010 *Opt. Express* **18** 19314
[22] Wang S and Wu H 2011 *Opt. Express* **19** 16259